



Dynamic Analysis of Folded Low Shells by Using Finite Element Analysis

Emmanuel E. T. Olodo^{1*}, Georges Adjibola A. Ale¹, Edmond Codjo Adjovi¹
and Antoine Vianou²

¹Laboratory of Energetic and Applied Mechanics (LEMA), University of Abomey-Calavi, 01BP2009,
Cotonou, Benin.

²Polytechnic School of Abomey-Calavi (EPAC), University of Abomey-Calavi, 01BP2009, Cotonou,
Benin.

Authors' contributions

This work was carried out in collaboration among all authors. All authors read and approved the final manuscript.

Article Information

DOI: 10.9734/CJAST/2020/v39i930611

Editor(s):

(1) Dr. S. Sathish, Hindustan Institute of Technology and Science, India.

Reviewers:

(1) Adel H. Phillips, Ain Shams University, Egypt.

(2) Ali Fadhil Naser, Al-Mussaib Technical College, Al Furat Al Awsat Technical University, Iraq.

(3) Carlos Fernando de Araújo Calado, University of Pernambuco, Brazil.

Complete Peer review History: <http://www.sdiarticle4.com/review-history/56732>

Received 26 February 2020

Accepted 01 May 2020

Published 13 May 2020

Original Research Article

ABSTRACT

Aims: This work is devoted to the development of a finite element algorithm for solving problem in forced vibrations of folded low shells.

Methodology: The differential equations for harmonic analysis are obtained from the Lagrange variational principle. Description of the dynamic behavior is made by the structure discretization into a system of curvilinear iso-parametric finite elements used in modal analysis. The method is implemented by a calculation code on a square-plane folded shell model with number of crease edges in both directions $k=l=3$.

Results: Displacement amplitudes are obtained by decomposition into vibration eigenforms. The maximum values of dynamic stresses are determined taking into account the shell's support conditions. The results of the harmonic analysis show that improvement in frequency characteristics and reduction of stresses in the folded shell depend on the constructive and internal damping of the structure and the increase in the number of fold edges k and l in both directions for example because this contributes to decrease in the forced vibration amplitudes.

*Corresponding author: E-mail: olodoe@live.fr;

Keywords: Forced vibrations; finite element algorithm; low shell.

1. INTRODUCTION

1.1 Study Background

Low shells are important structural elements widely used in various engineering applications such as industrial building covers, cultural, sports, etc. In these applications the shell structures may encounter vibrations and as a result may fail due to material fatigue. In the last decades, a huge amount of research efforts has been devoted to vibration analysis and dynamic behaviors of the shells and a larger variety of shell theories and computational methods have been proposed and developed by researchers.

1.2 Classical Approaches to Free and Forced Vibration Study of Low Shells

A comprehensive review on these can be found in [1]. This work includes comprehensive results of free vibration frequencies and mode shapes of shells subjected to different boundary conditions as well as detailed analysis of various shell theories. For vibration analysis of thin shells, classical shell theory has been used by many researchers [2-8]. Forced vibration of low shell with classical boundary condition is also of concern for a long time. Based on first order shear deformation theory, Khan et al. [9] performed the vibration analysis of clamped-clamped cylindrical shells using finite element method. Qu et al. [10] applied a domain decomposition technique to vibration problem of uniform and stepped cylindrical shells. Free and forced vibration of shell were examined under different boundary conditions and the forced response of shell was presented with different influence factors. Dai and Jiang [11] presented an analytical solution for forced vibration of a FGPM cylindrical shell and the effects of electric excitation, thermal load, mechanical load, and volume exponent on the static and dynamic behaviors were discussed. From the engineer's point of view, solving a vibration problem is the assessment of the damping properties of resonance pulsation Ω (or damping frequency) and modal damping η . The first approaches are analytical and rely in their entirety on various hypotheses to establish simplified differential equations. These can then easily be resolved using basic methods and allow the extraction of damping properties. However in real applications we face structures of various geometric and material configurations with varied limit conditions. The formulation of such problems

leads to complex equations that are difficult to solve with analytical methods. The only possible approach remains digital. In the literature, there are finite element models of all kinds, based on very different hypotheses [12,13].

1.3 Study Objectives

Some models are limited by the generated freedom degree number, others either by the geometric shape or the material configuration. This is the example of folded shell structures with a specified number of crease edges in both directions. However to our knowledge work related to the numerical study in forced vibrations of folded low shells is very little available in the technical literature.

In this work we propose an finite element algorithm for forced vibration problem solving of folded low shells by superimposing mode method taking into account the damping and constructive parameters of such structures.

2. MATERIALS AND METHODS

Folded shell will be modelled with use of isoparametric curvilinear quadrangle elements from the second order to eight nodes, with variable characteristics (Fig. 1).

The description of dynamic behaviour will be based on the lagrange variational principle [14]:

$$\frac{d}{dt} \left(\frac{\partial \exists}{\partial \dot{q}} \right) - \frac{\partial \exists}{\partial q} = F, \quad (1)$$

Here $\exists = \Pi - T$ is Lagrange's function,
 Π, T - the potential and kinetic energy of deformation and vibration of the shell,
 q - the nodal displacement vector of the finite element model,
 F - excitation loads.

Using the Lagrange's variational principle (1) we get the governing differential equation for harmonic analysis of the shell in matrix form. The finite element formulation of discrete equation of the movement of the structure taking into account damping can be expressed in the following matrix form:

$$[M] \left\{ \frac{d^2 q}{dt^2} \right\} + [C] \left\{ \frac{dq}{dt} \right\} + [K] \{q\} = \{F\}, \quad (2)$$

Or

$$[M] \{\ddot{q}\} + [C] \{\dot{q}\} + [K] \{q\} = \{F\},$$

$\{q\}$ -generalized nodal displacement vector;
 $\{\ddot{q}\}, \{\dot{q}\}$ - nodal acceleration vector and nodal velocity vector respectively;
 $[K], [C], [M]$ - the rigidity matrix, damping matrix and masse matrix respectively;
 $\{F\}$ - nodal excitation load vector.

In practice damping matrix is approximated by following relationship:

$$[C] = \alpha[M] + \beta[K]. \tag{3}$$

Remember that the equation of free vibrations without damping is of the following form:

$$(-\omega_i^2[M] + [K])\{q_0\}_i = \{0\} \tag{3a}$$

Knowing that for a conservative vibrational process all points of the structure move with the same frequency but with different phases, displacements can be expressed as follows:

$$\{q\} = \{q_0 e^{i\varphi}\} e^{i\Omega t} \tag{4}$$

q_0 - displacement amplitude
 Ω - external load pulse,
 t - time,
 φ - displacement phase.

For formulation of the problem in forced vibrations we will use complex notations. In this case expression (4) can be written in the following form:

$$\{q\} = \{q_0(\cos\varphi + i\sin\varphi)\} e^{i\Omega t} = (\{q_1\} + i\{q_2\}) e^{i\Omega t} \tag{5}$$

$\{q_1\} = \{q_0 \cos\varphi\}$ - real part of the displacement vector,
 $\{q_2\} = \{q_0 \sin\varphi\}$ - imaginary part of the displacement vector.

As external excitation load is periodic vector of dynamic charges can be expressed by Fourier's serie form:

$$\{F\} = \{F_0 e^{i\Omega t}\} e^{i\Omega t} = \{F_0(\cos \Psi)\} e^{i\Omega t} = (\{F_1\} + i\{F_2\}) e^{i\Omega t}, \tag{6}$$

F_0 - loading amplitude,
 ψ - loading phase,
 $F_1 = \{F_0 \cos\psi\}$ - real part of the force vector,
 $F_2 = \{F_0 \sin\psi\}$ - imaginary part of the force vector.

By substituting (5) and (6) into (2) we get:

$$(-\Omega^2[M] + \Omega[C] + [K])(\{q_1\} + i\{q_2\}) e^{i\Omega t} = (\{F_1\} + i\{F_2\}) e^{i\Omega t} \tag{7}$$

Or

$$([K] - \Omega^2[M] + \Omega[C])(\{q_1\} + i\{q_2\}) = (\{F_1\} + i\{F_2\}). \tag{8}$$

The problem (8) leads to the determination of the amplitude and load characteristics in forced vibrations and can be solved by the direct integration methods (central difference method, Wilson or Newmark method for example). However since these methods require considerable computational timewe have to use the superposition modemethod wich consist of decomposition the desired solution into eigenmodes to move on modal coordinates y_k by the following condition:

$$\{q\} = \sum_{k=1}^{\Theta} \{q_0\}_k y_k, \tag{9}$$

$\{q_0\}_k$ - vibration form of the k mode,
 Θ - considered mode number.

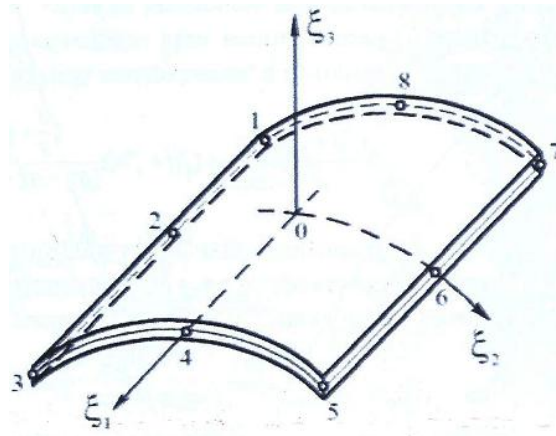


Fig. 1. Eight node Iso-parametric curvilinear element

By substituting expression (9) into equation (2) we get:

$$M \sum_{k=1}^{\theta} \{q_0\}_k \ddot{y}_k + C \sum_{k=1}^{\theta} \{q_0\}_k \dot{y}_k + K \sum_{k=1}^{\theta} \{q_0\}_k y_k = \{F\} \quad (10)$$

By multiplying equation (10) by the mode $\{q_0\}_j^T$ we get:

$$\{q_0\}_j^T M \sum_{k=1}^{\theta} \{q_0\}_k \ddot{y}_k + \{q_0\}_j^T C \sum_{k=1}^{\theta} \{q_0\}_k \dot{y}_k + \{q_0\}_j^T K \sum_{k=1}^{\theta} \{q_0\}_k y_k = \{q_0\}_j^T \{F\} \quad (11)$$

As previously stated M and K are orthogonal matrices [15,12].

For example for M matrix we have:

$$\{q_0\}_j^T M \{q_0\}_k = 0 \quad \text{if } k \neq j$$

And for K matrix we have:

$$\{q_0\}_j^T K \{q_0\}_k = 0 \quad \text{if } k \neq j \quad (12)$$

The mode superposition method involves:

$$\{q_0\}_j^T C \{q_0\}_k = 0 \quad \text{if } k \neq j \quad (13)$$

Applying conditions (12) and (13) to equation (11) we get the terms where $k=j$:

$$\{q_0\}_j^T M \{q_0\}_j \ddot{y}_j + \{q_0\}_j^T C \{q_0\}_j \dot{y}_j + \{q_0\}_j^T K \{q_0\}_j y_j = \{q_0\}_j^T \{F\}. \quad (14)$$

One can write also:

$$\{q_0\}_j^T M \{q_0\}_j = M_j q_{0j}^2 = 1, \quad (15)$$

From where we have: $q_{0j} = 1/\sqrt{M_j}$

Following [12] we have:

$$C_j = 2\eta_j \sqrt{K_j M_j}, \quad \omega_j = \sqrt{K_j / M_j}, \quad (16)$$

η_j - relative damping value for the j mode,

ω_0 - eigenpulse for the j mode.

So assuming the orthogonality of C taking into account (16) we get:

$$\{q_0\}_j^T C \{q_0\}_j = 2\eta_j \sqrt{K_j M_j} (1/\sqrt{M_j})^2 = 2\eta_j \omega_j. \quad (17)$$

By multiplying the equation (2.3a) by $\{q_0\}_j^T$ we get:

$$\{q_0\}_j^T K \{q_0\}_j = \omega_j^2 \{q_0\}_j^T M \{q_0\}_j. \quad (18)$$

Taking into account (15) equation (18) becomes:

$$\{q_0\}_j^T K \{q_0\}_j = \omega_j^2. \quad (19)$$

By substituting expressions (15), (17) and (19) into equation (14) we get a system of Θ independent motion equations for modal coordinates:

$$\ddot{y}_j + 2\eta_j \omega_j \dot{y}_j + \omega_j^2 y_j = F_j, \quad (20)$$

Here y_j is the modal coordinate;

F_j - load corresponding to the modal coordinate; $F_j = \{q_0\}_j^T \{F\}$.

For conservative harmonic vibrations F_j has the following form:

$$F_j = F_{0j} e^{i\Omega t} \quad (21)$$

F_{0j} - Load amplitude in complex form

Ω - external load pulsation.

The initial conditions for $y_j(t)$ are obtained from equality (9) and the following conditions:

$$\frac{\partial u_1}{\partial t} = \frac{\partial u_2}{\partial t} = \frac{\partial u_3}{\partial t} = \frac{\partial \theta_1}{\partial t} = \frac{\partial \theta_2}{\partial t} = 0 \quad (21a)$$

For equation (2.20) it is necessary to write the modal coordinate y_j in the same form as F_j in (21) i.e.:

$$y_j = y_{0j} e^{i\Omega t}, \quad (22)$$

Here y_{0j} amplitude of the modal coordinate j in complex form.

So taking into account (21) and (22) equation (20) becomes:

$$-\Omega^2 y_{0j} e^{i\Omega t} + 2\eta_j \omega_j (i\Omega y_{0j} e^{i\Omega t}) + \omega_j^2 y_{0j} e^{i\Omega t} = F_{0j} e^{i\Omega t} \quad (23)$$

By simplifying by $e^{i\Omega t}$ we get the following equation:

$$(-\Omega^2 + i2\Omega\eta_j\omega_j + \omega_j^2)y_{0j} = F_{0j} \quad (24)$$

Whose solving gives us:

$$y_{oj} = \frac{F_{oj}}{(\omega_j^2 - \Omega^2) + i(2\Omega\eta_j\omega_j)} \quad (25)$$

Knowing the modal coordinates can be determined the contribution of each mode in the solution:

$$\{C_j\} = \{q_0\}_j y_{oj} \quad (26)$$

$\{C_j\}$ - contribution of the j mode (displacement vector in complex form),
 $\{q_0\}_j$ - eigenmode j.

Having determined the values of y_j taking into account (23-26) and using the equation (9), we find the movements $\{q\}$.

Finally by suming up each of the modes, displacements can be determined in complex form:

$$\{q_0\} = \sum_{j=1}^{\theta} \{C_j\} \quad (27)$$

3. DETERMINATION OF THE DYNAMIC STRESS-STRAIN STATE

After determining the displacement amplitude values following (27) the stress-strain of the shell can be assessed. The behavior on the finite element average plane is described by the following relationship:

$$\{\sigma\} = \begin{Bmatrix} \sigma_{11} \\ \sigma_{22} \\ \sigma_{12} \end{Bmatrix} = [D_{\sigma}] \{\varepsilon\} = \frac{E}{1-\nu^2} \begin{bmatrix} 1 & \nu & 0 \\ \nu & 1 & 0 \\ 0 & 0 & \frac{(1-\nu)}{2} \end{bmatrix} \begin{Bmatrix} \varepsilon_1 \\ \varepsilon_2 \\ \varepsilon_3 \end{Bmatrix} \quad (28)$$

here $[D_{\sigma}]$ - the shell elasticity matrix.

Geometry of the shell average plane is given in global system of curvilinear coordinates $(\alpha_1, \alpha_2, \xi)$, ξ being the perpendicular coordinate to the shell average plane, α_1 , and α_2 coordinates

in the other two directions. Either $u_1(\alpha_1, \alpha_2)$, $u_2(\alpha_1, \alpha_2)$, $u_3(\alpha_1, \alpha_2)$ the components of the displacement vector on the shell average plane. The components of the elastic deformation tensor are given in the following form:

$$\begin{Bmatrix} \varepsilon_1 \\ \varepsilon_2 \\ \varepsilon_3 \\ \varepsilon_4 \\ \varepsilon_5 \\ \varepsilon_6 \end{Bmatrix} = \begin{Bmatrix} \frac{\partial u_1}{\partial \alpha_1} \\ \frac{1}{R} \left(\frac{\partial u_2}{\partial \alpha_2} + u_3 \right) \\ \frac{1}{R} \frac{\partial u_1}{\partial \alpha_2} + \frac{\partial u_2}{\partial \alpha_1} \\ \frac{\partial^2 u_3}{\partial \alpha_1^2} \\ -\frac{1}{R} \left(\frac{1}{R} \frac{\partial^2 u_3}{\partial \alpha_2^2} - \frac{\partial u_2}{\partial \alpha_2} \right) \\ \frac{1}{R} \left(\frac{\partial \alpha_1}{\partial \alpha_1} - \frac{\partial^2 u_3}{\partial \alpha_1 \partial \alpha_2} \right) \end{Bmatrix} \quad (29)$$

R- curvature radius of the hull.

The dynamic stresses will be determined by taking into account (5), (28) and (29). The exposed mathematical model allows analysis of the stress and deformation distribution for given vibration frequencies and forms.

4. RESULTS AND DISCUSSION

The object structure of the study is a square-plan folded shell with the mathematical model presented in Fig. 2. The crease edge number in both directions is $k=l=3$.

Shell is discretized by a mesh consisting of 1600 elements and 1640 nodes (Fig. 3).

- Limit conditions. Two types of boundary conditions are considered: CCCC and SSSS conditions.
- Initial conditions. They are given by:

$$\text{For } t=0, \frac{\partial u_1}{\partial t} = \frac{\partial u_2}{\partial t} = \frac{\partial u_3}{\partial t} = \frac{\partial \theta_1}{\partial t} = \frac{\partial \theta_2}{\partial t} = 0 \quad (30)$$

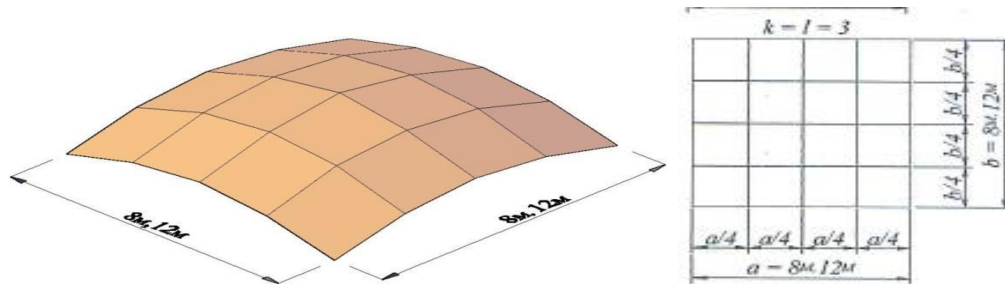


Fig. 2. Mathematical model of folded shell

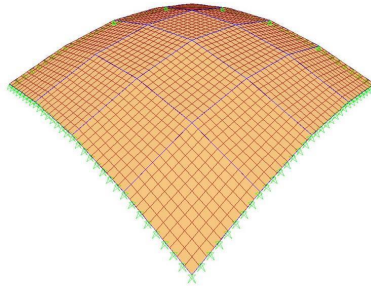


Fig. 3. Folded shell mesh

On the other hand, the hull is subjected to a harmonic frequency load $\Omega_1 = 14,1 \cdot 10^3 s^{-1}$. The excitation load amplitude is $F_0 = 0,12 MPa$.

deflections with SSSS-type boundary conditions. We see that the maximum values of u_3 are observed at the first resonance.

Fig. 4 shows the variations curves of the deflections u_3 according to the coordinate α_1 .

Fig. 5 reports the results of calculation of normal displacements in forced vibrations ($\bar{\Omega} = \Omega_i/\omega_0$) according to internal damping, where $\bar{\Omega}$ is a frequency parameter, Ω the frequency of forced vibrations, ω_0 the resonance frequency.

Fig. 4(1) characterizes the distribution of u_3 deflections with CCCC boundary conditions, while Fig. 4(2) shows the distribution of

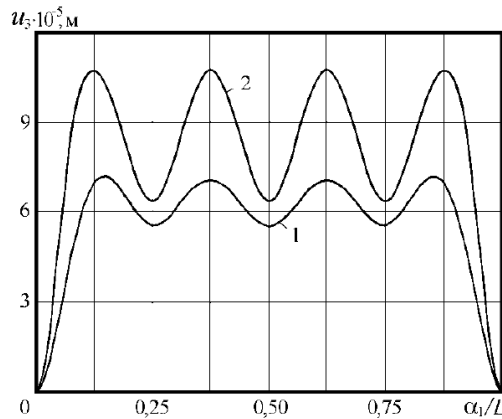


Fig. 4. Deflection variation curve u_3 according to coordinate α_1
 1- CCCC boundary conditions
 2- SSSS boundary conditions

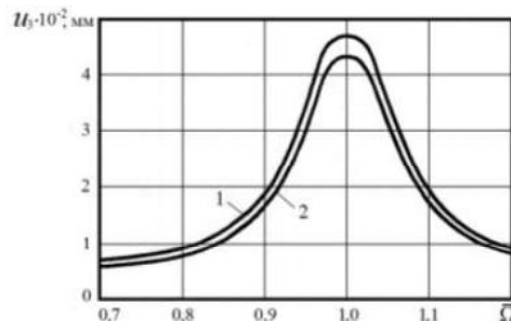


Fig. 5. Forced Vibration amplitudes with damping
 1- CCCC boundary conditions
 2- SSSS boundary conditions

The considered damping coefficient is $\eta = 0,06$, the excitation frequency is $\Omega_2 = 7,759 \cdot 10^3 s^{-1}$. Fig. 5(1) corresponds to the CCCC clamped shell, while Fig. 5(2) corresponds to the SSSS simply supported shell. On these curves it is observed that the maximum amplitude is reached on the resonance frequency and then its value decreases rapidly. It can also be seen that the amplitude values of the CCCC shell are higher than that of the SSSS shell, however we can see that the difference between these values is hardly considerable.

Fig. 6 shows the frequency characteristics curves of the clamped shell with different values of the damping coefficients.

It can be seen on these curves that when the damping coefficient value increases amplitude maximum value decreases. It should be noted that forced vibration amplitude gradually

increases with increase in vibration frequency. When one reaches the resonance frequency one observes a sudden increase and then a gradual decrease in displacement amplitude. Knowledge of eigen frequencies prevents resonance appearing in a frequency range by increasing the mechanical rigidity of the system. This reduces the variable component of dynamic forces that is the main excitation source.

In Fig. 7, acceleration variations in the central section of folded shell are reported.

The maximum and minimum acceleration values for both shell types are $1,75 m/s^2$ and $-1,64 m/s^2$ for the CCCC shell, $1,25 m/s^2$ and $-1,15 m/s^2$ for the SSSS shell respectively. The maximum acceleration of the clamped is greater than that on simple support. This shows the influence of the support mode on forced vibration amplitude of the shell.

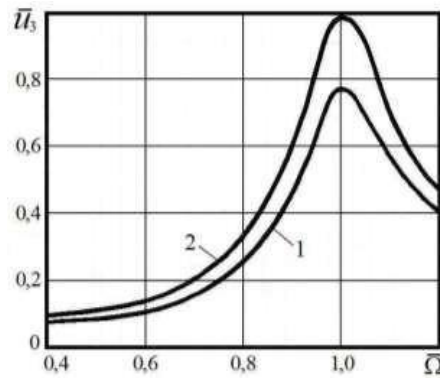
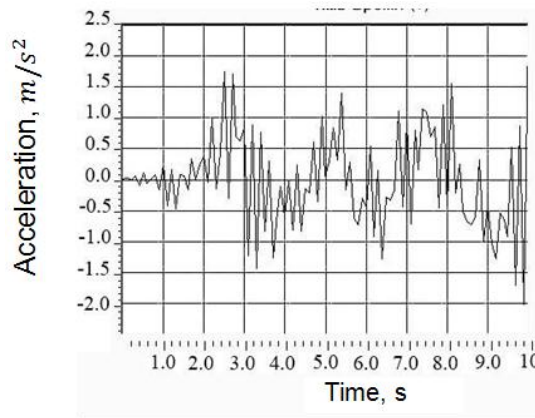


Fig. 6. Curves of the frequency characteristics of forced vibrations

- 1- Damping coefficient $\eta = 0,06$
- 2- Damping coefficient $\eta = 0,03$



a)

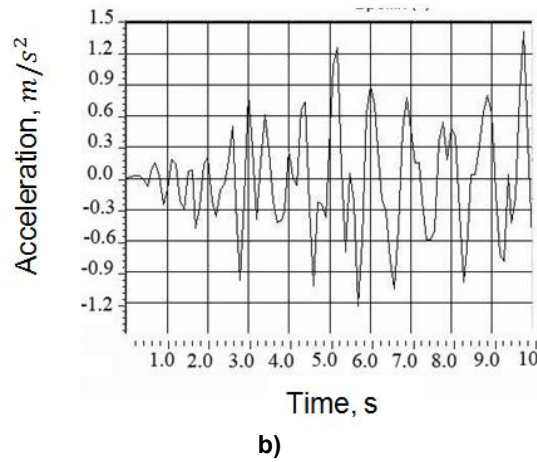


Fig. 7. Acceleration variation curves in the central section of the shell

- a- CCCC boundary conditions
- b- SSSS boundary conditions

Table 1. Maximum and minimum acceleration values of the central section

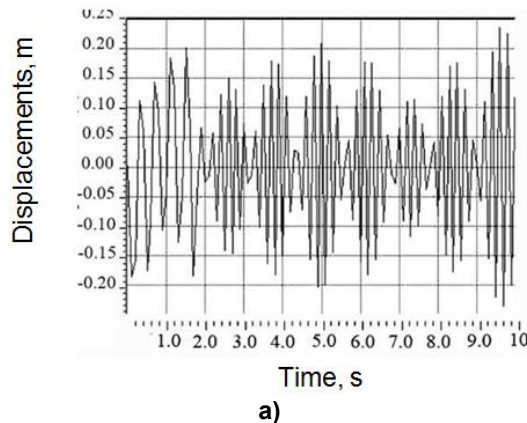
Shell type	Acceleration, m/s^2	
	Max	Min
CCCC shell	1,75	-1,64
SSSS shell	1.25	-1.15

Fig. 8 shows vertical displacement curves in the central section for both shell types depending on the considered boundary conditions.

The maximum and minimum displacements are 0.23 m and -0.23 m respectively for the clamped shell, 0.140 m and -0.141 m for the simply supported shell. We can see that the maximum displacement in the central section of the clamped shell is greater than that of the shell on simple support. This also shows influence of the support mode on deflections in the central section of folded shell.

Fig. 9 shows the stress distribution in the central section of the two shell types according to the considered boundary conditions.

The maximum and minimum values of normal stresses in the central sections are 2,132 MPa and -0,0928 MPa respectively for clamped shell, 0,940 MPa and -0.023 MPa for the simply supported shell. It can be seen that the maximum value of the dynamic normal stress in the central section of the simply supported shell is greater than that of the clamped shell. The results of the harmonic analysis show that improvement in frequency characteristics and reduction of stresses in the folded shell depends on the constructive and internal damping of the structure by increasing, for example, the number of fold edges k and l in both directions as this contributes to the decrease in the forced vibration amplitude.



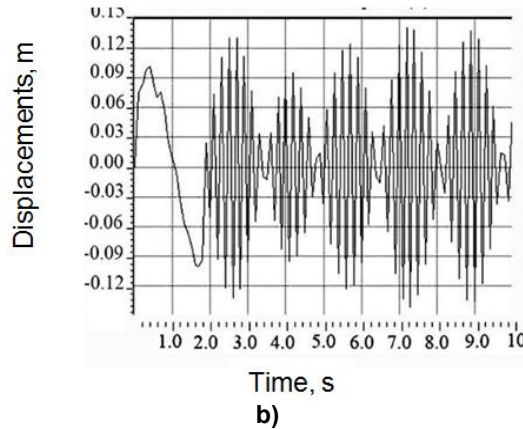


Fig. 8. Vertical displacements in folded shell central section
 a- CCCC shell
 b- SSSS shell

Table 2. Vertical displacements in the central section

Shell type	Vertical displacements, m	
	Max	Min
CCCC shell	0.23	-0.23
SSSS shell	0.140	-0.141

Table 3. Normal stress in the central section

Shell type	σ_{max} (MPa)	σ_{min} (MPa)
CCCC shell	2,132	-0,0928
SSSS shell	0,940	-0,023.

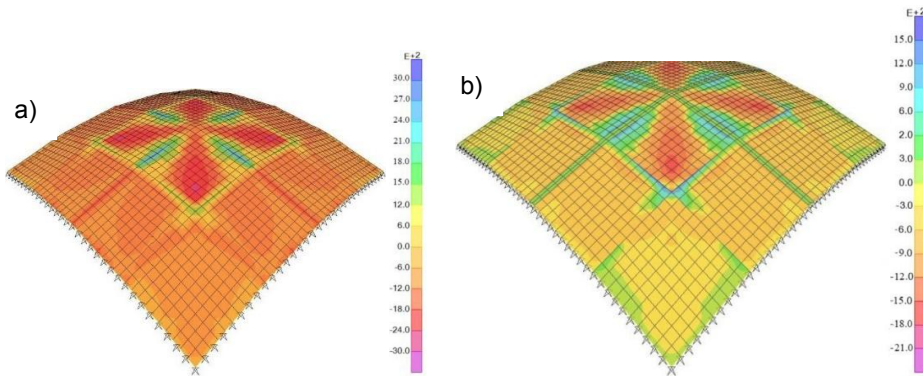


Fig. 9. Distribution of the dynamic stresses in the central section of folded shell
 a- CCCC shell
 b- SSSS shell

5. CONCLUSION

In this work we can conclude that a mathematical model of dynamic behaviour and stress-strain state of folded low shells has been developed. Taking into account the constructive characteristics related to the number of fold edges and the size. The following main results are:

- A finite element algorithm is developed for the forced vibration analysis of low folded shell.
- Differential equations for harmonic analysis of shells are obtained based on the Lagrange variational principle.
- Description of the dynamic behaviour of the low shells is made by structure discretization into a system of curvilinear

iso-parametric finite elements used in modal analysis.

- The displacement amplitudes are obtained by decomposition into vibration eigenforms.
- The proposed mathematical model is developed by the superposition mode method taking into account damping and constructive parameters.
- The maximum values of dynamic stresses are determined, taking into account the shell support conditions.

These results can serve as theoretical basis for the analysis and numerical calculation of frequency characteristics and stress for this class of structures subject to dynamic loadings.

COMPETING INTERESTS

Authors have declared that no competing interests exist.

REFERENCES

1. Subrata K, Reza K. Dynamic analysis in three layered conical shells utilising numerical methods. *Int J Hydr.* 2018;1(4): 427-446.
2. Trung T, Van K, Pham B, Van M, Van T, Hoang N. Forced vibration analysis of laminated composite shells reinforced with graphene nanoplatelets using finite element method. *Adv Civ Eng.* 2020;1:1-17.
3. Valle J, Albanesi A, Fachinotti V. An general cylindrical coordinates finite element method for dynamic study of thickness-independent shells. *Lat Am J Struct.* 2019;16(5):1-26.
4. Emad H, Reza A, Jalal T. Nonlinear forced vibration analysis of FG-CNTRC cylindrical shells under thermal loading using a numerical strategy. *Int J. App Mech.* 2017;9(8):1750108.
5. Franca DO, Pedrosa LJ. Study of dynamic behavior in cylindrical shell coupled with fluid. *Proc IASS An Symp., Spain, Barcelona;* 2019.
6. Melian L, Cho WST. Engineering dynamics and vibration; vibration and nonlinear dynamics of plates and shells – applications of flat triangular finite element. *Bentham Science;* 2018.
7. Dogan A. Dynamic response of laminated composite shells under various impact loads. *Mech Time Dep Mat.;* 2019. DOI: 10.1007/s11043-019-09434-z
8. Sofiyev A. The vibration and stability behavior of freely supported FGM conical shells subjected to external pressure. *Comp Struc.* 2009;89:356-366.
9. Khan K, Patel B, Nath Y. Free and forced vibration characteristics of bimodular composite laminated circular cylindrical shells. *Comp Struc.* 2015;126:386–397.
10. Qu Y, Chen Y, Long X, Hua H, Meng G. Free and forced vibration analysis of uniform and stepped circular cylindrical shells using a domain decomposition method. *App Acou.* 2013;74(3):425–439.
11. Dai H, Jiang H. Forced vibration analysis for a FGPM cylindrical shell. *Sho Vib.* 2013;20(3):531–550.
12. Bathe K. Finite element procedures in engineering analysis. *Prentice-Hall;* 1982.
13. Johnson C, Kienholz D. Finite element prediction of damping in structures with constrained viscoelastic layers. *Amer Ins Aer Astr.* 1982;20:1284-1290.
14. Zienkiewicz C. The finite element method. 5th Ed *Oxford: Butterworth-Heinemann Linacre House, Jordan Hill;* 2000.
15. Wilkinson J. The algebraic eigenvalue problem. *Oxford University Press;* 1988.

© 2020 Olodo et al.; This is an Open Access article distributed under the terms of the Creative Commons Attribution License (<http://creativecommons.org/licenses/by/4.0>), which permits unrestricted use, distribution, and reproduction in any medium, provided the original work is properly cited.

Peer-review history:

The peer review history for this paper can be accessed here:
<http://www.sdiarticle4.com/review-history/56732>